Development of the FAST Code for Modelling CANDU Fuel

A. Prudil[1], B.J. Lewis and P. Chan
Chemistry and Chemical Engineering Department,
Royal Military College of Canada,PO Box 17000, Kingston, Ontario, Canada

Abstract

The Fuel And Sheath modelling Tool (FAST) is a general purpose fuel performance code for normal operating conditions developed at RMC. FAST includes models for heat generation and transport, thermal-expansion, elastic strain, densification, fission product swelling, contact, grain growth, fission gas release, gas and coolant pressure and sheath creep. These models have been coupled together using the Comsol platform and are solved on a quarter cross-section of a fuel pellet and sheath in two dimensions (radial-axial). FAST has undergone a preliminary validation against experimental post-irradiation data from six fuel elements and comparison to the ELESTRES-IST and ELESIM fuel performance codes. The results show excellent agreement with experimental measurements and other codes.

1. Introduction

Nuclear fuel design is a key component of the design of new reactors and has been considered to mitigate reactor aging phenomena (e.g. modified37 element bundle). Since the number of in situ fuel tests are limited by the high economic cost and difficulty associated with performing in-reactor measurements, modelling tools have been developed to help bridge the gaps between experimental results.

Nuclear-fuel modelling codes have always been limited by the computing resources available at the time. This has historically restricted fuel modelling codes to one-dimensional and quasi-two-dimensional representations of fuel-elements to reduce the computation expense of the models to manageable levels. In the time since these models were created, advancements in both computer hardware and software have expanded modelling capabilities beyond previous limitations. This advancement has made feasible more computationally expensive models which require fewer simplifying assumptions and provide more accurate results than those previously available. For instance, fully coupled multiphysicsmodelling approaches have been used at to develop multi-dimensional fuel performance codes[1–4]. This work builds on this approach to produce a fully-coupled two-dimensional (radial-axial) model including detailed fuel pellet and sheath geometries and improved contact phenomena.

2. Model Development

Understanding the behaviour of nuclear fuel during irradiation is a complicated multi-physics problem involving neutronics, chemistry, radiation physics, material-science, solid-mechanics, heat-

transfer and thermal-hydraulics. In the following subsectionsthe separate effects models used in the FAST code have been summarized. The material property models aretaken from AECL, MATPRO as available open journal publications.

2.1 Heat Generation & Transport

The primary requirement of any fuel modelling code is to determine the temperature, T, throughout the fuel element because most material properties are temperature dependent and many phenomena are thermally driven. Heat transport in fuel elements operating under normal conditions occurs primarily by conduction.This process is modelled by the heat-conduction equation:

$$\rho C_p \frac{\partial T}{\partial t} = \nabla \cdot (k \nabla T) + Q_{prod} \tag{1}$$

where ρ, C_p and k are the material properties of density, specific heat capacity and thermal conductivity, respectively. The volumetric heat production rate, Q_{prod}, accounts for heat deposited in the fuel pellet. In practice, the material properties in Equation (1) are not constants; they are dependent on many factors such as temperature, porosity, burnup, grain size, phase, radiation damage and/or manufacturing conditions. Empirical and semi-empirical correlations for these material properties are used to account for these dependencies where they are significant.

The volumetric heat generation term is assumed to be proportional to the neutron flux profile in the fuel pellet. The flux distribution in the element is dependent on the initial composition, size and density of the fuel, as well as the current burnup distribution of the fuel and the neutron spectrum of the reactor. For fuel modelling purposes, the flux profile is calculated from correlations developed from reactor physics and/or Monte-Carlo codes. The model employed in this work is that used in the ELESTRES-IST codes, where the volumetric heat generation term is given by

$$Q_{prod} = f_{mag}\left(I_0\left(\kappa_{flux} r\right) + \beta_{flux}\, \mathrm{e}^{\lambda_{flux}(r-P_r)}\right) \tag{2}.$$

Here f_{mag} is a proportionality coefficient to achieve the required average linear power for the element, I_0 is the zeroth order modified-Bessel function of the first kind, r is the radial coordinate, P_r is the pellet radius, and the parameters κ_{flux}, β_{flux}, and λ_{flux} are the flux depression parameters derived and tabulated from the reactor physics codes.

Heat conduction across the pellet-to-sheath gap requires a special treatment due to the high aspect ratio for the given geometry. The code uses aone-dimensional (1-D) steady-state heat transport model developed by Campbell et al., in which the heat flux in the radial direction, Q_r, in W m^{-2}, is given by

$$Q_r = \left(\frac{k_g}{1.5\left(R_f + R_s\right) + d_{gap} + g_s + g_f} + \left(\frac{2k_f k_s}{k_f + k_s}\right)\frac{P_i}{a_0\sqrt{d_{gap}}H}\right)\left(T_{fuel} - T_{sheath}\right) \tag{3}.$$

Here the first term accounts for the conduction through the gas in the gap and the second term accounts for solid-to-solid contact between the surfaces. The variables k_g, k_f and k_s are the thermal conductivity of the gas, the fuel and the sheath, respectively (all in units of W m^{-2} K^{-1}). In the first term, the average local gap distance is denoted by d_{gap}.The surface roughness of the fuel and sheath materials as well as the temperature jump distances, which are R_f,R_s,g_s and g_f respectively, increase the effective size of gap to account for the imperfect heat transfer at the solid-to-gas interface. For the solid-to-solid conductance term, a_0 is a constant with a value of $8.6 \cdot 10^{-9}$ $m^{0.5}$ $Pa^{0.5}$, P_i is the local average contact pressure at the interface (Pa) and H is the Meyer hardness of the Zircaloy in (Pa). In the case of an open gap, the contact pressure is zero and the solid conduction term does not contribute.

2.2 Deformation Mechanics

In the reactor, the geometry of the fuel elements deforms as a result of a number of processes including: mechanical loading, thermal-expansion, material creep, fuel densification and fission product swelling. The strains caused by these are divided into three types: thermal, elastic and plastic. In this model, it is assumed that the net deformation can be calculated as the sum of the individual strains.

2.2.1 Thermal Strain

The expansion of a material due to a change in temperature is known as thermal expansion. The magnitude of the change in size is characterized by the thermal expansion coefficient,α_p, which is the strain per degree of temperature. Using this definition, the strain in a material due to thermal expansion, ε_{thm}, can be approximated as

$$\varepsilon_{thm} = \alpha_P \left(T - T_0 \right) \tag{4}$$

where T is the temperature and T_0 is the reference temperature for which the thermal strain is assumed to be zero.

2.2.2 Elastic Deformation

The elastic strains were calculated using the Hookean model of elasticity. According to this model,the linear strain, ε, and the shear strain, γ, are proportional to the applied load. The linearly elastic model is usually condensed to strain-vector and elasticity-matrix notation as

$$\begin{bmatrix} \varepsilon_x \\ \varepsilon_y \\ \varepsilon_z \\ \gamma_{xy} \\ \gamma_{xz} \\ \gamma_{yz} \end{bmatrix} = \begin{bmatrix} 1/E_x & -\nu_{xy} & -\nu_{xz} & 0 & 0 & 0 \\ -\nu_{yx} & 1/E_y & -\nu_{yz} & 0 & 0 & 0 \\ -\nu_{zx} & -\nu_{zy} & 1/E_z & 0 & 0 & 0 \\ 0 & 0 & 0 & 1/G_{xy} & 0 & 0 \\ 0 & 0 & 0 & 0 & 1/G_{xz} & 0 \\ 0 & 0 & 0 & 0 & 0 & 1/G_{yz} \end{bmatrix} \begin{bmatrix} \sigma_x \\ \sigma_y \\ \sigma_z \\ \tau_{xy} \\ \tau_{xz} \\ \tau_{yz} \end{bmatrix} \quad (5)$$

where, E, ν and G is are the Young's modulus, Shear modulus and Poisson's ratio of the materials. The subscripts indicate the appropriate direction vectors.Although it is known that the elastic properties of the fuel sheath are not isotropic, this effect was ignored because the total elastic strains are small compared to the plastic deformations which result from the effect of creep[5].

2.2.3 Contact

In the FAST code, the contact between the pellet and sheath is modelled using the penalty method (pellet-to-pellet contact is not considered). This method allows the contact surfaces to pass through each other and applies a pressure to each surface as a function of penetration depth to push them apart. Using this method thesteady-state penetration depth can be made to an arbitrarily low level by using a stiff (large) penalty function. However, high contact stiffness can decrease the stability of the solution because it increases the sensitivity of the solution to small changes in displacement. A value of the penalty function was selected which limits penetration to several microns which is small enough to not significantly affect the results.

2.2.4 Pellet Densification

Densification is a process by which the density of the UO_2 fuel increases under irradiation by removal of porosity from the fuel, resulting in negative strains. When in the reactor, the UO_2 fuel will continue to sinter due to high temperatures, pressures and radiation effects.This phenomenon causes volumetric strain equal to

$$\varepsilon_{vol,dens} = \frac{\Delta V_{dens}}{V_0} = \frac{1-p_0}{1-p_0(1-F)} - 1 \quad (6)$$

where p_0 is the initial porosity and F is the fraction of initial porosity which has been removed from the fuel which is calculated using an empirical correlation developed by Hastings[6]. The correlation is

$$F = 0.6 - \exp\left(-0.506 - 8.67\times10^{-10}T^3\left(1-\exp\left(-2.867\times10^{-2}Bu\right)\right)\right) \quad (7)$$

whereBu is the burnup of the fuel in MW h kgU^{-1}. According to this model, the fraction of initial porosity which can be removed from the fuel saturates at 60%.

2.2.5 Fission Product Swelling

UO_2 fuel experiences a swelling effect due to the buildup of fission product atoms in the fuel. The swelling effect is divided into two sources: solid fission product swelling and gaseous fission product swelling.

The solid-fission product swelling occurs because the space occupied by two fission product atoms in the fuel matrix is greater than the space occupied by a single UO_2 atom. The volumetric strain due to solid fission product swelling is assumed to be linearly proportional to the fuel burnup. Olander reports a volumetric strain of

$$\varepsilon_{vol,SFP} = 0.0032\frac{Bu}{225} \tag{8}$$

where Bu is the burnup in units of MWh kgU^{-1}[7,8].

The gaseous fission product swelling is caused by the formation of fission gas bubbles on the grain boundaries. The MATPRO[8] correlation for the volumetric strain rate of the gaseous fission products, $\varepsilon_{vol,GFP}$, in units of s^{-1} in differential form is calculated by

$$\frac{d(\varepsilon_{vol,GFP})}{dt} = 9.42\left(10^{-36}\right)(2800-T)^{11.73}e^{\left[-0.0162(2800-T)-8.0\left(10^{-27}\right)Buf\right]}\frac{dBuf}{dt} \tag{9}.$$

Here Buf is the fuel burnup measured by number of fissions per unit volume. The volumetric strain from fission gas swelling is then calculated by the time integral of Equation (9).

The MATPRO model also recommends that the gaseous swelling rate at temperatures below 1000 K be set to zero as it assumed that the fission products do not diffuse from the grain at a sufficient rate to produce significant swelling. Similarly, above 2000 K MATPRO assumes that the swelling stops because the fission gas bubbles are able to escape from the fuel.

2.2.6 Sheath Creep

Creep is a type of time-dependent plastic deformation that occurs at elevated temperatures and at stress levels below the yield stress of the material. Three types of creep are known to occur in CANDU fuel sheaths each resulting from different mechanisms. These were modeled using the work of Holt, Hosbons and Coleman[5]of AECL as a function of a parameter known as the equivalent stress. Although this model was developed for temperatures above 700 K, it is being extrapolated and applied to lower temperatures as experienced during normal operating conditions due to lack of an available model for CANDU fuel in the open literature.

The equivalent stress is a measure of the total stress at a point due to combined loads in different directions:

$$\sigma_{eqv} = F_{Hill}\left(\sigma_\phi - \sigma_z\right)^2 + G_{Hill}\left(\sigma_z - \sigma_r\right)^2 + H_{Hill}\left(\sigma_r - \sigma_\phi\right)^2 \tag{10}$$

where σ_r σ_ϕ and σ_z are the stress in the r, ϕ and z directions, respectively. The coefficients F_{Hill}, G_{Hill} and H_{Hill} are known as the Hill anisotropy parameters. These parameters are assumed to be equal to the as-fabricated values which are F_{Hill}=0.773, G_{Hill}=0.532 and H_{Hill}=0.195.

Creep due to grain-boundary sliding occurs when the boundaries between crystals, which are weakly bonded, slide past each other due to the applied load. The expression for the strain rate for this type of creep in units of s^{-1} is given by

$$\frac{d\varepsilon_{gb}}{dt} = 6.34 \cdot 10^{-6} \left(\frac{\sigma_{eqv}}{G g_d} \right)^2 \exp\left(\frac{-9431}{T} \right) \tag{11}$$

where, G is the shear modulus of the sheath in Pa, g_d is the average grain diameter in m, T is the temperature in K and σ_{eqv} is the equivalent stress in Pa.

The second type of creep is known as dislocation creep or dislocation glide. This type of creep occurs when crystallographic dislocations (which are imperfections in the crystal structure) move. The creep rate which results from this process, $\epsilon_{d,}$ in units of s^{-1}, is determined by solving the coupled equations

$$\frac{d\sigma_{int}}{dt} = 0.016E \left(\frac{d\varepsilon_d}{dt} \right) \left(1 - \frac{\sigma_{int}}{0.33\left(\sigma_{eqv} - \sigma_{int} \right)} \right) \tag{12}$$

$$\frac{d\varepsilon_d}{dt} = C_d \exp\left(\frac{-34726}{T} \right) \sigma_{int}^{5.3} \tag{13}.$$

The internal stress field, σ_{int}, represents the retarding effect of crystallographic dislocations on the creep rate, E is the Young's modulus in units of Pa, and C_d is a constant with a value of $C_d = 2.98 \cdot 10^{-28}$ s^{-1} $Pa^{-5.3}$.

A third creep mechanism, called transition creep, occurs when the material undergoes a phase transition while under stress. This type of creep requires minimum temperatures that do not occur during normal operating condition and was therefore not included in the version of FAST for normal operating conditions.

The creep rate in the primary directions is found from the total creep rate distributed according to the plastic flow rule for anisotropic materials. Applying the plastic flow rule, we obtain the creep in each of the primary directions as follows

$$\begin{bmatrix} \varepsilon_r \\ \varepsilon_\phi \\ \varepsilon_z \end{bmatrix} = \int_0^t \frac{d\varepsilon_{creep}}{dt} \frac{1}{\sigma_{eqv}} \begin{bmatrix} G_H + H_H & -H_H & -G_H \\ -H_H & H_H + F_H & -F_H \\ -G_H & -F_H & G_H + F_H \end{bmatrix} dt \tag{14}.$$

The result was then applied to the solid-mechanics by adding the creep strains to the elastic and thermal strains.

2.3 Fission Gas Release Calculation

The release of fission gas from irradiated UO_2 fuel to the free volume in the element is a very complicated phenomenon. The model used in this thesis is based on the models employed by Morgan[1] and Shaheen[2–4]. The release process is modeled in two steps. In the first step, fission gas is produced in the fuel grains and diffuses to the grain boundary, where it accumulates. The second step occurs when the fuel grain surface becomes saturated and any additional fission gas at the grain surface is released to the free volume of the element.

2.3.1 Release to the Grain Boundaries

The fission gas release to the fuel grains can be modelled by Booth diffusion of the fission gas to the fuel surface[1,2,9–11]. In this model, the fuel grains are treated as idealized homogenous spheres from which the fission gas atoms diffuse. The fission gas is produced uniformly throughout each of the spheres which are assumed to be initially free of the gas. The grain surface is assumed to be a perfect fission gas sink (i.e. concentration on the grain surface is assumed to be zero). The gas is assumed to diffuse throughout the solid fuel matrix according to Fickian diffusion (where the particle flux is proportional to the concentration gradient),and released from the surface of the idealized grain.

This grain diffusion model was implemented numerically at 26evenly spaced radial positions within the fuel pellet and the results interpolated between these points. At each radial location, a 1-D radially symmetric finite-element model of the concentration profile in the UO_2 grain was produced using the relevant local temperature, fission rate and grain size. This numerical implementation was benchmarked against the analytic solution to this model published by both Kidson[12]and by Rim[13]. These analytic solutions are developed by discretization of the timehistory into periods over which the diffusion coefficient, grain size and fission gas production rate are constant. The benchmark was comprised of a step increase in temperature at the mid-point of the irradiation. It showed excellent agreement between the analytically and numerically derived solutions. The numerical solution was found to be easier to implement since the time discretization is performed by time-dependent solver in Comsol.

The fission rate density necessary for this calculation was found from the volumetric rate of heat productionand the thermal energy released per fission. It was assumed that the fission gas yield per fission is approximately 0.251 atom fission^{-1}and the energy released per fission is approximately 200 MeV fission^{-1}.

The average local UO_2grain size was determined by solving the grain growth relationship provided by Khoruzhii et al.[14]. The rate of grain growth is given as

$$\frac{dg_d}{dt} = 1.46\left(10^{-8}\right)\exp\left(\frac{-32100}{T}\right)\left(\frac{1}{g_d} - \frac{\exp\left(\frac{7620}{T}\right)}{2.23\times10^{-3}} - \frac{F_{rate}T\exp\left(\frac{5620}{T}\right)}{6.71\times10^{18}}\right) \quad (15).$$

Here T is the temperature in K and F_{rate} is the fission rate density.Note that this model does not consider the distribution of grain sizes within a region; it only considers the average grain size. In the thesis work of Shaheen, it was shown that this simplification produces good results for fission gas release despite potentially wide variations in the grain-size distribution[2].

The diffusion coefficient for fission gas in UO_2 was obtained from Morgan[1] who followed the work of Turnbull *et al.*[15–17] and White & Tucker[11].

2.3.2 Gas Release to the Fuel Element

Once fission gas has been released to the grain surface it becomes trapped in intergranular bubbles between fuel grains. The release of fission gas from the grain boundary to the element occurs when sufficient fission gas has accumulated between grains to allow the bubbles to interlink and form a path to the surface through the intergranular porosity and cracks. The amount of gas required at the grain surface to achieve inter-linkage is called the grain-boundary saturation (or critical swelling).

The two-stage release process effectively contains a portion of the fission gas, G_b, in intergranular bubbles even after the bubbles have been interlinked. This is because if there is not sufficient fission gas to maintain the interlinked network, the bubbles become isolated and cannot release gas to the bulk of the element. From this theory, the release rate from the grain boundary from a small fuel volume, dV, is

$$\frac{\partial R_e}{\partial V} = \begin{cases} R_{gb} - \dfrac{\partial G_{bsat}}{\partial t} & G_b \geq G_{bsat} \\ 0 & G_b < G_{bsat} \end{cases} = \mathrm{H}\left(G_b - G_{bsat}\right)\left(R_{gb} - \frac{\partial G_{bsat}}{\partial t}\right) \quad (16)$$

whereH is the Heaviside (unit step) function. The number of moles of fission gas atoms released to the element, R_e, can then be calculated by integrating over the volume. The contribution from the time derivative of the grain boundary saturation allows a for time-dependent grain-boundary saturation. The grain boundary saturation in gas atoms per cubic meter is dependent on the temperature and grain diameter (g_d) according to

$$G_{bsat} = \frac{2.03\cdot10^{23}}{Tg_d} \quad (17).$$

This relationship can result large increase in the rate of gas released to the element volume due to an increase in temperature when the grain boundary is already saturated.

2.4 Gas Pressure Calculation

The internal gas pressure is calculated using the non-homogenous temperature form of the ideal gas law. This is given by

$$P = \frac{nR_{gas}}{\int_V \frac{1}{T} dV} \tag{18}$$

where n is the number of moles of gas within the element, R_{gas} is the ideal gas constant, T is the temperature of the gas in K and V is the volume occupied by the gas. In the model, the gas volume is divided into five sub-volumes which are all calculated individually and added together. The sub volumes are the pellet-to-sheath gap, the pellet-to-pellet gap, the UO_2 crack volume, and the element ends (or plenum). Since the gaseous regions are not meshed, the temperature in the regions has been approximated using the temperatures on the boundaries of the gas volumes.

3. Validation

A limited proof of concept validation was undertaken to test the model under realistic physical conditions. Using irradiation history, manufacturing information and Post-Irradiation Examination (PIE) measurement data for a number of irradiated UO_2fuel elements was used to validate FAST. The PIE data includes average and maximum measurements of the elemental gas volume, mid-pellet diameter change, mid-pellet sheath strain, sheath ridge height at pellet-to-pellet interface and sheath ridge strain. The measured values of these parameters were compared to the predictions of the FAST code. Results from ELESTRES and ELESIM code simulations were also included in the comparison to establish a baseline for the accuracy of existing fuel-modeling codes.

For most of the irradiation cases, multiple fuel elements were irradiated and measured for each case history. These elements are from the same concentric rings of a fuel bundle. Cases 3-6 are from the same fuel bundle, but positioned in different rings and thus would experience a different neutron flux (linear power) for each ring.

The cases selected for this validationcover a range of power and burnup conditions as well as a number of geometries. The maximum burnup, maximum linear power, burnup averaged linear power and time-averaged linear power for each of the elements are listed in Table 1.

The results of the PIE comparison have been summarized in a series of graphs which show the results for all the cases simultaneously. The case number has been used as the x-coordinate for these graphs. The average experimental value has been included along with the maximum measured value for each element, where available. This provides a scale for the scatter in the experimental results.

The graph shown in the left side of Figure 1 shows the mid-pellet diametrical change of the sheath. In these results, we can see that in all cases the experimental measurements of mid-pellet deformation is greater than the predicted values. In all cases except for number 1, the FAST code

predicts greater deformation than both ELESTRES and ELESIM, bringingit closer to the measured deformation.

The predicted height of the circumferential ridgesis shown in the right side of Figure 1. Both FAST and ELESTRES are able to predict average ridge height within the scatter of the data. As a general trend, FAST appears to systematically underestimate the ridge height while ELESTRES overestimates it in all but one case. It is believed that the systematic underpredictionin FAST may be due to the lack of a UO_2 creep model which would increase the plastic strains in the UO_2 and consequently contribute to a larger ridge height.

Table 1: Fuel element power history information for PIE comparison.

Case	Num Element per Bundle	Num Pellets Per Element	Max Burnup (MWh kgU^{-1})	Max Power (kW m^{-1})	Time Average Power (kW m^{-1})
1	37	31	132	37	30
2	28	26	302	53	31
3	37	31	552	41	32
4			455	34	26
5			405	30	24
6			385	29	23

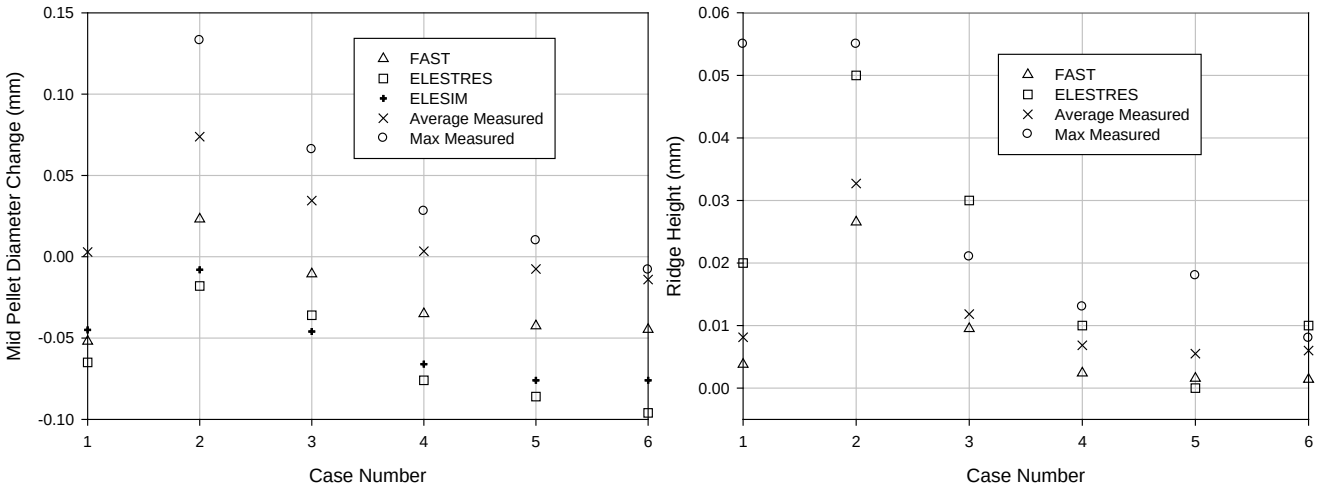

Figure 1: Results of simulation of PIE element results for FAST validation. **Left:**Comparison of mid-pellet diameter change.**Right:** Comparison of circumferential ridge height.

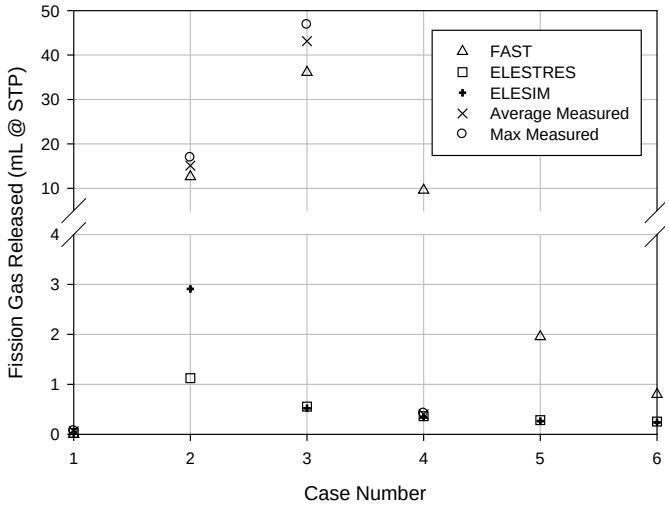

Figure 2: Comparison of measured fission gas release to model predictions at end of life.

The fission gas release measurements are compared to the predicted values in Figure 2. Note that only cases 1-4 included measured fission gas volumes as no fission-gas measurements were made for cases 5 and 6 (very little fission gas release is expected for these cases). For the cases with significant gas release (cases 2 and 3), FAST appears to agree quite well with the experimental data. For cases with less fission gas release, FAST appears to overestimate the release. In these cases, ELESTRES appears to be better able to predict the release volumes.

4. Conclusion

The FAST code is a general purpose fuel performance code with an emphasis on the modeling of the deformation of the fuel pellet and sheath. FAST is a collection of separate effects models which have been coupled together and are solved simultaneously using the Comsol finite-element Multiphysics platform. The code includes models for deformation due to thermalexpansion, elastic strain, densification and swelling of the fuel, contact forces, internal gas pressure, external coolant pressure, as well as two sources of creep in the sheath. The temperature distribution in the fuel element is calculated, including a flux depressed fission heating of the fuel pellet and one-dimensional models for the pellet-to-sheath gap and sheath-to-coolant heat-transfer. The pellet model includes models for the grain growth of UO_2 and a two-stage fission gas release model. The sheath includes anisotropic models for thermalexpansion and creep.

This code includes some improvements from previous modelling at RMC, including a more detailed pellet geometry, localized pellet-to-sheath gap size and contact pressure, localized fuel burnup, a two-dimensional finite element model (FEM) to simulate deformation of the sheath, models for material properties, a FEM Booth-diffusion model (including an ability to model transient release effects), and a capability for end-of-life predictions.The FAST code has been validated through both code-to-code comparisons with ELESTRES-IST and ELESIM models and with the available experimental fuel performance data. It has been demonstrated to successfully model the end-of-life condition including sheath circumferential ridging effects. Overall, it is expected that the FAST

code will prove to be a useful and adaptable tool to support further development of CANDU fuel design and improved modelling tools.

5. Acknowledgements

The authors would like to acknowledge the support of our colleagues at RMC, as well as S. Yatabe and M.R. Floyd (AECL) for providing validation data. Funding for this work was provided by NSERC, UNENE and COG through the Industrial Research Chair (IRC) program and an ORF grant.

6. References

[1] D. Morgan, "A thermomechanical model of CANDU fuel," MASc Thesis, Royal Military College of Canada, Kingston, Ontario, 2007.
[2] K. Shaheen, "A mechanistic code for intact and defective nuclear fuel element performance," Royal Military College of Canada, Kingston, Ontario, 2011.
[3] K. Shaheen, J. S. Bell, A. Prudil, and B. J. Lewis,, "Modelling CANDU Fuel Element and Bundle Behaviour for Performance of Intact and Defective Fuel," in *Proceedings of the International Conference on the Future of Heavy Water Reactors*, Ottawa, Ontario, 2011.
[4] K. Shaheen and B. J. Lewis, "Platform-Based Modelling of Intact and Defective Fuel Behaviour," in *Proceedings of Top Fuel 2009 Conference*, Paris, France, 2009.
[5] H. E. Sills, "ELOCA: Fuel element behavior during high-temperature transients." Chalk River Nuclear Laboratories, Atomic Energy of Canada Limited, Mar-1979.
[6] I. J. Hastings and L. E. Evans, "Densification Algorithm for Irradiated UO2 Fuel," *Journal of the American Ceramic Society*, vol. 62, no. 3-4, pp. 217-218, 1979.
[7] D. Olander, *Fundamental Aspects of Nuclear Reactor Fuel Elements*. Us Dept of Energy, 1976.
[8] SCDAP/RELAP5 Development Team, "Volume IV: MATPRO -- A Library of Material Properties for Light-Water-Reactor Accident Analysis," Idaho National Engineering and Environmental Laboratory, Idaho Falls, Idaho, NUREG/CR-6150 INEL-96/0422, Oct. 1997.
[9] A. El-Jaby, "A model for predicting coolant activity behavior for fuel-failure monitoring analysis," PhD Thesis, Royal Military College of Canada, Kingston, Ontario, 2009.
[10] S. Beck, "The Diffusion of Radioactive Fission Products from Porous Fuel Elements," Battelle Memorial Institute, Columbus, Ohio, BMI-1433, Apr. 1960.
[11] R. J. White and M. O. Tucker, "A new fission-gas release model," *Journal of Nuclear Materials*, vol. 118, no. 1, pp. 1-38, Aug. 1983.
[12] G. V. Kidson, "A generalized analysis of the cumulative diffusional release of fission product gases from an 'Equivalent Sphere' of UO2," *Journal of Nuclear Materials*, vol. 88, no. 2-3, pp. 299-308, Feb. 1980.
[13] Rim et al., "Background and Derivation of ANS-5.4 Standard Fission Product Release Model," American Nuclear Society, NUREG/Cr-2507, Jul. 1981.
[14] O. V. Khoruzhii, S. Y. Kourtchatov, and V. V. Likhanskii, "New model of equiaxed grain growth in irradiated UO2," *Journal of Nuclear Materials*, vol. 265, no. 1-2, pp. 112-116, Feb. 1999.
[15] J. A. Turnbull, C. A. Friskney, J. R. Findlay, F. A. Johnson, and A. J. Walter, "The diffusion coefficients of gaseous and volatile species during the irradiation of uranium dioxide," *Journal of Nuclear Materials*, vol. 107, no. 2-3, pp. 168-184, Jun. 1982.
[16] C. A. Friskney, J. A. Turnbull, F. A. Johnson, A. J. Walter, and J. R. Findlay, "The characteristics of fission gas release from monocrystalline uranium dioxide during irradiation," *Journal of Nuclear Materials*, vol. 68, no. 2, pp. 186-192, Oct. 1977.
[17] J. A. Turnbull, C. A. Friskney, F. A. Johnson, A. J. Walter, and J. R. Findlay, "The release of radioactive gases from uranium dioxide during irradiation," *Journal of Nuclear Materials*, vol. 67, no. 3, pp. 301-306, Aug. 1977.